

# Periodically Nonuniform Coupled Microstrip-Line Filters With Harmonic Suppression Using Transmission Zero Reallocation

Sheng Sun, *Student Member, IEEE*, and Lei Zhu, *Senior Member, IEEE*

**Abstract**—In this paper, the two-port periodically nonuniform coupled microstrip line with finite length is thoroughly studied as an equivalent  $J$ -inverter network for microstrip bandpass filters with harmonic suppression. Extracted  $J$ -inverter susceptance is exhibited to vary up and down versus frequency with the null or transmission zero when the coupled length becomes half-wavelength. This transmission zero can be adjusted by varying the periodicity and/or slit depth to suppress the first spurious harmonic passband of the filter. Firstly, two one-stage bandpass filters with wide and narrow bandwidths are designed to assure the first-harmonic passband is fully suppressed as illustrated in theory and experiment. Secondly, a three-stage bandpass filter with harmonic suppression is designed optimally. The predicted  $S$ -parameters are found in good agreement with the measured values, at least 40-dB insertion loss, at the point where the first-harmonic passband is achieved.

**Index Terms**—Bandpass filter, harmonic suppression,  $J$ -inverter network, periodically nonuniform microstrip coupled line, transmission zero.

## I. INTRODUCTION

COUPLED microstrip lines have been widely used as promising coupling elements in the design of bandpass filters due to several attractive features such as compact size, low profile, and tightened capacitive coupling [1], [2]. However, these microstrip bandpass filters with uniform coupled microstrip-line sections usually suffer from the spurious passband at the second resonant frequency of the microstrip-line resonator. Consequently, it makes the upper stopband performance worse. As is well known today, it is predominantly caused by the nonsynchronous feature of even- and odd-mode velocities of propagation in the inhomogeneous dielectric medium. To circumvent this problem, much effort has been made thus far to equalize the phase velocities of even and odd modes by differentiating their traveling routes [3]–[13]. Initially, a simple over-coupled coupled microstrip-line section is formed in [3] to compensate for the difference in phase velocity between these two dominant modes. Alternatively, the nonuniform coupled microstrip line with multiple cascaded sections [4] is made and the dielectric substrate is mechanically

suspended above the ground plane [5], [6] to achieve phase compensation.

In recent years, much more interest has been aroused to utilize the periodically nonuniform coupled microstrip line, with various unit-cell configurations as a simple and effective approach to address this problematic issue. The sinusoidal modulation on the widths of two strip conductors [7] and the corrugated coupled-slot structure [8], [9] are formulated to extend the actual odd-mode traveling path toward its even-mode counterpart at the first-harmonic passband. Similarly, the squared grooves are periodically and symmetrically etched out at both sides of the coupled lines [10]. The split ring resonators are also periodically placed in the proximity of the parallel strip conductors [11]. In [12], the meander coupled microstrip line is constructed with reduced size. In addition, the aperture is periodically formed on the ground plane to equalize the even/odd-mode phase velocities in the design of the wide-band bandpass filters by making use of its tight coupling [13]. Without knowing the even- and odd-mode characteristic impedances and phase velocities of these periodically nonuniform coupled microstrip lines, all the above filters can only be designed optimally. This is done by executing the direct electromagnetic simulation of these electrically large overall layouts at the cost of intensive CPU time and huge memory.

In fact, if the frequency-dispersive coupling performance of these periodically nonuniform coupled microstrip lines is comprehensively investigated, the task of designing these filters may be easily accomplished using the efficiently network-based synthesis approach [1], [2]. Recently, the effective per-unit-length transmission parameters of infinite-extended periodically nonuniform coupled microstrip lines have been extracted in [14] to demonstrate the frequency-dispersive and slow-wave behavior of even and odd dominant modes via a hybrid full-wave method-of-moments (MoM) and short-open calibration (SOC) procedure, namely, the MoM-SOC. In this study, the two-port periodically nonuniform coupled microstrip line with finite length is characterized as an equivalent  $J$ -inverter network, showing its frequency-dispersive coupling performance, and reallocating the transmission zero toward suppressing the first-harmonic passband of coupled microstrip-line filters. Two one-stage bandpass filters are designed, fabricated, and measured to quantitatively demonstrate that the first-harmonic resonance can be fully suppressed for both tight and weak coupling cases. From a designed example, a three-stage bandpass filter

Manuscript received October 15, 2004; revised December 24, 2004.

The authors are with the School of Electrical and Electronic Engineering, Nanyang Technological University, Singapore 639798 (e-mail: ezhul@ntu.edu.sg).

Digital Object Identifier 10.1109/TMTT.2005.847079

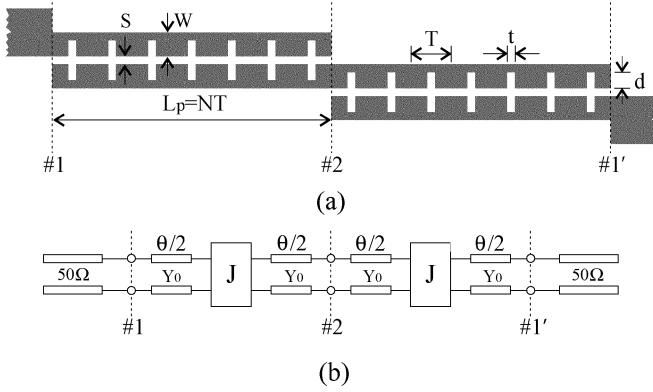


Fig. 1. Physical layout and equivalent network for one-stage bandpass filter. (a) Physical layout. (b) Equivalent-circuit network.

is built and predicted  $S$ -parameters are well assured by our experiment over a frequency range.

## II. PRINCIPLE OF HARMONIC SUPPRESSION

### A. One-Stage Bandpass Filter

Fig. 1(a) depicts the geometry of a one-stage bandpass filter, which is constructed by cascading the two identical quarter-wavelength periodically nonuniform coupled microstrip-line sections at the central interface (#2). In this aspect, a number of rectangular slits or notches [14] are periodically etched out in the inner edges of the two strip conductors. By adjusting the number and dimension of these slits properly, the even- and odd-mode phase velocities may be equalized at the second resonance of the middle resonator. As shown in Fig. 1(a), each length ( $L_P = NT$ ) consists of finite periodical cells ( $N$ ) with the periodicity ( $T$ ) and slit width/depth ( $t$  and  $d$ ), whereas  $W$  and  $S$  are the widths of the two strips and coupling gap. Its equivalent circuit network is described in Fig. 1(b). Each section is modeled as a  $J$ -inverter network with the susceptance ( $J$ ) at the center and two equal electrical lengths ( $\theta/2$ ) at the two sides. As studied in the uniform coupled microstrip-line case [15], the distributed  $J$ -susceptance has been shown to vary as a quasi-periodical function of frequency. It reaches the peak and null values at the frequencies of  $\theta/2 = 90^\circ$  and  $\theta/2 = 180^\circ$ , respectively.

### B. Equivalent $J$ -Inverter Network

As detailed in [14], the characteristic impedances ( $Z_{0e}, Z_{0o}$ ) and phase constants ( $\beta_e, \beta_o$ ) of the periodically nonuniform coupled microstrip line can be first effectively extracted using our developed full-wave MoM-SOC technique. As a result, this allows one to derive the two-port impedance ( $Z$ ) matrix of the open-circuited periodically nonuniform coupled microstrip-line section with the length of  $L_p = NT$  in terms of even- and odd-mode per-unit-length parameters of a generalized coupled transmission line in an inhomogeneous medium in such a closed form [16] as follows:

$$Z_{11} = Z_{22} = \frac{-j}{2} (Z_{0e}^h \cot \beta_e L_p + Z_{0o}^h \cot \beta_o L_p) \quad (1)$$

$$Z_{12} = Z_{21} = \frac{-j}{2} (Z_{0e}^h \csc \beta_e L_p - Z_{0o}^h \csc \beta_o L_p). \quad (2)$$

The superscript  $h$  indicates half a symmetrical coupled microstrip-line case in conjunction with the definition in [1] and [2]. Due to the different definitions of wave current and voltage quantities in the modeling of the whole and half asymmetrical coupled microstrip line, the above two sets of even- and odd-mode characteristic impedances can be explicitly related as

$$Z_{0e}^h = 2Z_{0e} \quad (3)$$

$$Z_{0o}^h = \frac{Z_{0o}}{2}. \quad (4)$$

Equations (1) and (2) imply that each element in the  $Z$ -matrix is purely imaginary and they can be converted into the relevant admittance ( $Y$ ) matrix with the two independent susceptances of  $B_{11} = B_{22}$  and  $B_{12} = B_{21}$ . Under the equivalence of two matrices or networks for the same periodically nonuniform coupled microstrip-line block, the  $J$ -susceptance ( $J$ ) and electrical length ( $\theta$ ) can be expressed as [15]

$$\bar{J} = \frac{\tan\left(\frac{\theta}{2}\right) - \bar{B}_{11}}{\bar{B}_{12} \tan\left(\frac{\theta}{2}\right)} \quad (5)$$

$$\theta = n\pi + \tan^{-1} \left\{ \frac{2\bar{B}_{11}}{1 - \bar{B}_{11}^2 + \bar{B}_{12}^2} \right\} \quad (6)$$

where  $\bar{J} = J/Y_0$ ,  $\bar{B}_{11} = B_{11}/Y_0$ ,  $\bar{B}_{12} = B_{12}/Y_0$ ,  $n$  is an integer number, and  $Y_0$  is the characteristic admittance of the uniform lines that excite the open-circuited periodically nonuniform coupled microstrip line at the two sides.

### C. Frequency-Dispersive $J$ -Inverter Network Parameters

As the infinitely long periodically nonuniform coupled microstrip line is modeled via MoM-SOC, as done in [14], the two  $J$ -inverter network parameters can be calculated using (1)–(6). Fig. 2(a) and (b) describes the three sets of normalized  $J$ -inverter susceptance ( $\bar{J}$ ) and electrical line length ( $\theta/2$ ) versus frequency under three different depths of rectangular slits, i.e.,  $d = 0.00$  (uniform case), 0.36, and 0.50 mm. In comparison with the approximate assumption of no frequency dispersion, the dispersive coupling performance of this periodically nonuniform coupled microstrip line is characterized as a simple equivalent  $J$ -inverter network. As seen in Fig. 2(a), the parameter  $\bar{J}$  increases quickly, reaches the peak, falls down to the null, and then goes up again. It exhibits a nonmonotonous and quasi-periodical coupling behavior as a function of frequency. The coupling degree at the frequency  $f_a^0$ ,  $f_b^0$ , or  $f_c^0$  becomes null, thus, it brings out the transmission zero in the  $S$ -parameters.

The electrical line length ( $\theta/2$ ) at the two sides of the  $J$ -susceptance is found to quasi-linearly go up from  $33^\circ$  to  $273^\circ$  as the frequency increases from 1.0 to 7.0 GHz. From Fig. 1(a) and (b), it can be figured out that the middle transmission-line resonator is actually formed by cascading two identical electrical lengths ( $\theta/2$ ). Its overall length is equal to  $\theta$ . Intuitively, the transmission-line resonator resonates at the frequencies of  $\theta = 180^\circ, 360^\circ, 540^\circ$ , etc. The first resonance happened at  $\theta = 180^\circ$ , and is usually utilized to make up the dominant passband in the design of a bandpass filter. The second resonance at  $\theta = 360^\circ$

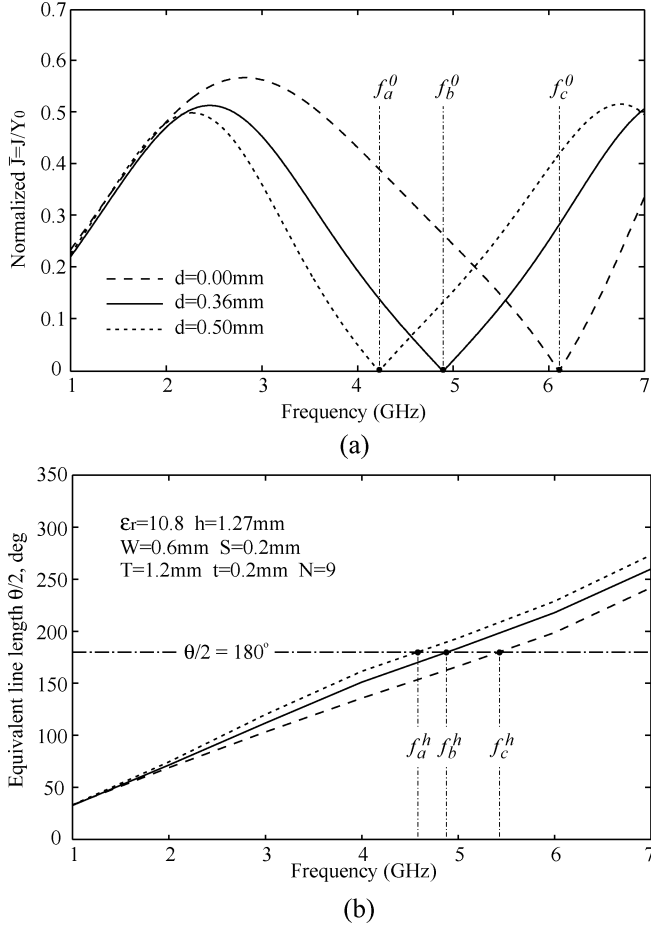


Fig. 2. Frequency-dispersive  $J$ -inverter network parameters with respect to different slit depths. (a) Normalized  $J$ -susceptance. (b) Electrical line length.

$[\theta/2 = 180^\circ$  in Fig. 2(b)] contributes to the first-harmonic spurious passband with central frequencies, i.e.,  $f_a^h$ ,  $f_b^h$ , or  $f_c^h$ , in conjunction with the three different slit depths ( $d$ ), as shown in Fig. 2(b). In fact, these three depths ( $d$ ) are simultaneously expressed in Fig. 2(a) and (b) to comparatively demonstrate the three distinctive cases about the relationships between the transmission zero and first-harmonic resonance frequencies, i.e.,

$$\begin{cases} f_a^0 < f_a^h, & d = 0.50 \text{ mm} \\ f_b^0 = f_b^h, & d = 0.36 \text{ mm} \\ f_c^0 > f_c^h, & d = 0.00 \text{ mm} \end{cases} \quad (7)$$

where superscripts 0 and  $h$  indicate the transmission zero and first-harmonic resonance cases, respectively.

#### D. Transmission Zero Reallocation

To consider the tight and weak coupling cases, as requested in the multiple-stage bandpass filter, both the transmission zeros and harmonic resonant frequencies, and also the frequency quantities  $f^0$  and  $f^h$  are plotted in Fig. 3(a) and (b) with respect to the slit depth ( $d$ ) for  $S = 0.2$  mm and 0.6 mm, respectively. By adjusting the slit depth ( $d$ ) under the pre-selected periodicity ( $T$ ), these two curves or lines are intercepted with each other at a certain frequency where  $f^0 = f^h$ . Furthermore, as shown in Fig. 3, the intersection point occurs

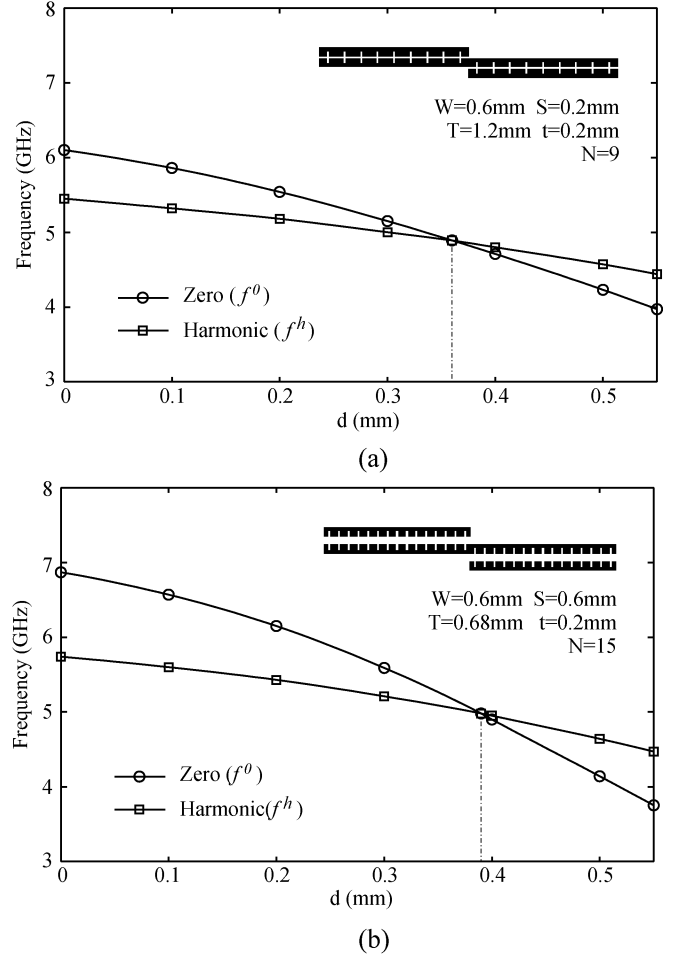


Fig. 3. Frequency of transmission zero and harmonic resonance versus the depth of transverse slit. (a) Tight coupling with  $S = 0.2$  mm. (b) Weak coupling with  $S = 0.6$  mm.

at  $d = 0.36$  mm for the tight coupling case with  $S = 0.2$  mm and  $T = 1.2$  mm, whereas it appears at  $d = 0.39$  mm for the weak coupling case with  $S = 0.6$  mm and  $T = 0.68$  mm.

Of course, this interception point may also be generated and then reallocated to the particular frequency by reducing the periodicity ( $T$ ) or increasing the unit number ( $N$ ) for a fixed coupled length ( $L_p$ ) properly. Table I tabulates the two frequency quantities ( $f^0$  and  $f^h$ ) with respect to the unit number ( $N$ ). The former one largely exceeds the latter one and decreases in a faster manner to meet up with the latter one at  $N = 9$  where  $f^0 = f^h = 4.9$  GHz. As demonstrated later, these two equalized frequencies provide us with a direct and effective approach in canceling or suppressing the first-harmonic spurious passband in filter design.

#### E. Harmonic-Resonance Cancellation

Let us study the frequency response of the one-stage bandpass filter in Fig. 1(a) and demonstrate whether the first-harmonic resonance can be cancelled via the transmission zero reallocation technique presented above. Fig. 4 depicts the frequency responses of transmission coefficient ( $|S_{21}|$ ) for the one-stage bandpass filter with the three different slit depths listed in (7). As the transmission zero is exactly reallocated to its relevant

TABLE I  
FREQUENCY OF TRANSMISSION ZERO AND HARMONIC RESONANCE VERSUS THE NUMBER OF FINITE CELLS UNDER THE FIXED COUPLED LENGTH ( $L_P$ )

N	0	1	2	3	4	5	6
$f^0$	6.1	5.96	5.81	5.66	5.52	5.38	5.25
$f^h$	5.45	5.37	5.3	5.23	5.16	5.10	5.05
N	7	8	9	10	11	12	13
$f^0$	5.12	5.01	4.9	4.78	4.68	4.58	4.48
$f^h$	4.99	4.94	4.9	4.84	4.80	4.78	4.75

Frequency unit: gigahertz; substrate:  $\epsilon_r = 10.8$ ,  $h = 1.27$  mm;  $W = 0.6$  mm,  $S = 0.2$  mm,  $t = 0.2$  mm,  $L_P = 10.8$  mm

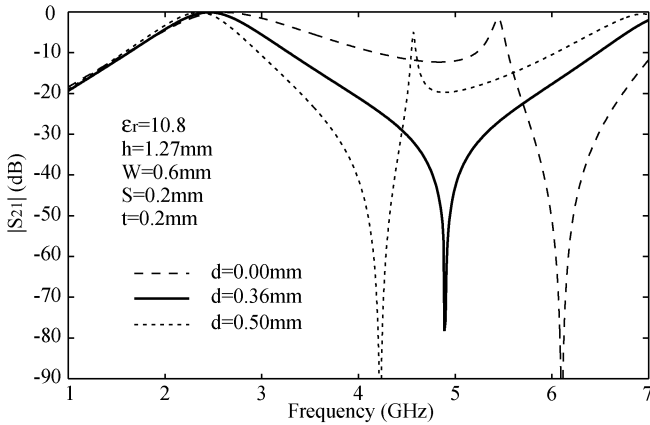


Fig. 4. Frequency responses of one-stage bandpass filters with different slit depths under the fixed coupled length ( $L_P = 10.8$  mm) and periodicity ( $T = 1.2$  mm).

resonant frequency, i.e.,  $f^0 = f^h$  ( $d = 0.36$  mm), the transmission pole can be cancelled to a great extent. Otherwise, the transmission pole and zero appear separately at the two unequal frequencies in the other two cases in conjunction with  $d = 0$  and  $0.50$  mm. As a result, the appearance of these transmission poles will damage the stopband performance, as can be observed in Fig. 4.

Furthermore, the frequency response of this one-stage bandpass filter is investigated versus a different slit number ( $N$ ) under the fixed depth ( $d$ ) and physical length ( $L_P$ ). The simulated results are illustrated in Fig. 5. On the basis of the derived parameters in Table I, the finite cell number ( $N$ ) is selected as 0, 5, 9, and 13. This will take into account all the three distinctive cases, as summarized in (7), as well as the uniform case with  $N = 0$ . At  $N = 0$ , the frequency at the minimum  $|S_{21}|$  appears around 6.1 GHz. It is brought out by the transmission zero ( $f^0$ ), as given in Table I. It is much higher than that at the maximum  $|S_{21}|$ , i.e., first-harmonic resonant frequency ( $f^h = 5.45$  GHz). As  $N$  enlarge to five, the two frequencies of the transmission zero and pole are shifted downward in different extents, thereby reducing their discrepancy ( $f^0 - f^h$ ) from 0.65 to 0.28 GHz. At  $N = 9$ , the zero is reallocated to its pole, i.e.,  $f^0 - f^h = 0$  GHz. Thus, the concerned pole or first-harmonic resonance is completely

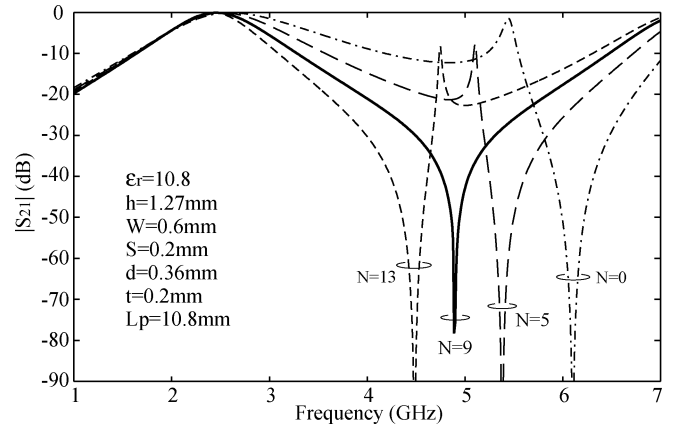
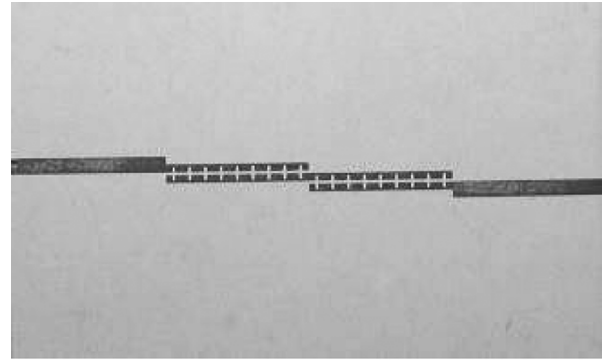
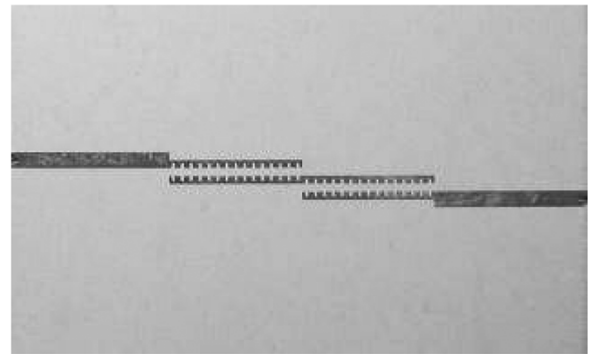


Fig. 5. Frequency responses of one-stage bandpass filters with different numbers of finite cells under the fixed coupled length ( $L_P = 10.8$  mm).



(a)



(b)

Fig. 6. Two fabricated one-stage bandpass filters. (a) Tight coupling. (b) Weak coupling.

suppressed, as illustrated via the solid line in Fig. 5. When  $N$  further increases to 13, the pole emerges again at the frequency ( $f^h = 4.75$  GHz) higher than its zero at  $f^0 = 4.48$  GHz. It can be observed in Fig. 5.

### III. FILTER DESIGN: PREDICTED AND MEASURED RESULTS

On the basis of the above discussion, the two extreme cases with tight and weak coupling are considered initially to make up the two one-stage bandpass filters with harmonic suppression at their first-order spurious passbands. Fig. 6(a) and (b) shows the photographs of the two fabricated filters with narrow and wide coupling gap widths ( $S$ ), respectively. Our design goal is

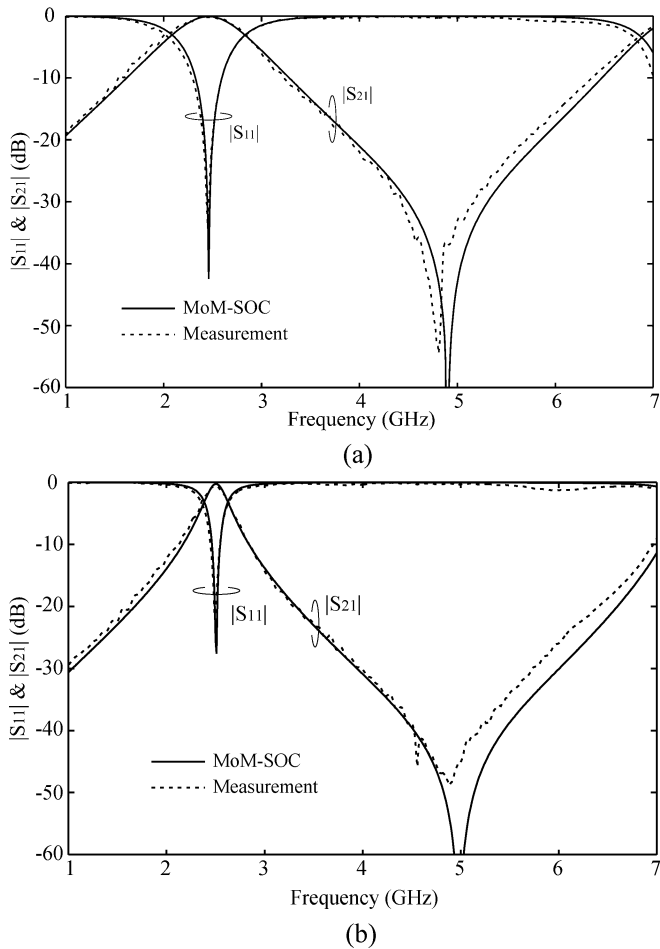


Fig. 7. Predicted and measured  $S$ -parameters of the one-stage bandpass filters that are shown in Fig. 3. (a) Tight coupling with  $S = 0.2$  mm. (b) Weak coupling with  $S = 0.6$  mm.

to achieve identical dominant resonant frequencies at 2.45 GHz while canceling the first-harmonic resonance in both cases. We need to find the proper values for the periodicities and slit depths according to the results in Fig. 3 and Table I. Measured results are plotted together with the predicted results in Fig. 7(a) and (b), giving an evident confirmation that the first-harmonic resonances are completely suppressed in both tight and weak coupling cases.

With the innovative use of these periodically nonuniform coupled microstrip lines, a multistage bandpass filter with first-harmonic suppression will be able to be constructed in reality. In a design example, a three-stage bandpass filter is designed optimally. The photograph of the fabricated sample is shown in Fig. 8. The tightly coupled section is arranged at the input and output. The weakly coupled one is put at the middle sections. In comparison with the symmetrical geometry of the second resonator, the first and third resonators are constructed by cascading the two dissimilar periodically nonuniform microstrip-line sections. The predicted and measured  $S$ -parameters are plotted in Fig. 9, showing a good agreement with each other in the frequency region from 1.0 to 7.0 GHz. The measured results illustrate that the return loss achieves approximately 20 dB in the whole dominant passband

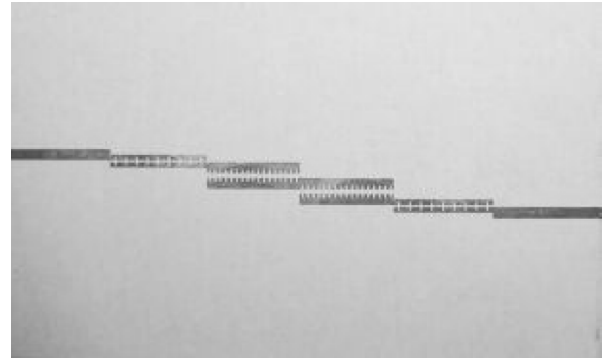


Fig. 8. Fabricated three-stage bandpass filter.

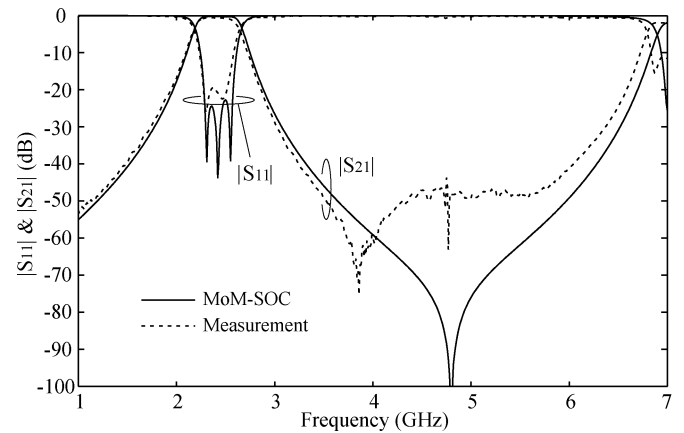


Fig. 9. Predicted and measured  $S$ -parameters of the three-stage bandpass filter. (Tight-coupling section:  $W = 0.6$  mm,  $S = 0.2$  mm,  $T = 1.2$  mm,  $d = 0.38$  mm, and  $N = 9$ . Weak-coupling section:  $W = 1.18$  mm,  $S = 0.5$  mm,  $T = 0.6$  mm,  $d = 0.45$  mm, and  $N = 17$ .)

at around 2.45 GHz. The insertion loss is higher than 40 dB at the first-harmonic passband located at around 4.90 GHz.

#### IV. CONCLUSION

This study has examined the periodically nonuniform coupled microstrip lines with finite length in terms of a generalized coupling-oriented  $J$ -inverter network. It does exhibit the basic principle of suppressing the first-harmonic passband in the filter design with the use of the transmission zero reallocation technique. Extensive results have demonstrated that the transmission zero or  $J$ -susceptance null of the periodically nonuniform coupled microstrip line can be reallocated to cancel the first-harmonic resonance. This is done by adjusting the periodicity and/or loaded slit dimension properly. The two one-stage bandpass filters are designed and fabricated to provide an initial support on the proposed technique for the periodically nonuniform coupled microstrip line with tight and weak coupling. Lastly, a three-stage bandpass filter is designed optimally and its predicted results are evidently assured from our experiment.

#### ACKNOWLEDGMENT

The authors sincerely appreciate S. Y. Chua, DSO National Laboratories, Singapore, for his support in measurement and K.

H. Lui, Nanyang Technological University, Singapore, for his help in proofreading the manuscript.

#### REFERENCES

- [1] D. M. Pozar, *Microwave Engineering*, 2nd ed. New York: Wiley, 1998.
- [2] J. S. Hong and M. J. Lancaster, *Microstrip Filters for RF/Microwave Applications*. New York: Wiley, 2001.
- [3] A. Riddle, "High performance parallel coupled microstrip filters," in *IEEE MTT-S Int. Microwave Symp. Dig.*, vol. 1, 1988, pp. 427–430.
- [4] S. Denis, C. Person, S. Toutain, B. Théron, and S. Vigneron, "Parallel coupled microstrip filter with phase difference compensation," *Electron. Lett.*, vol. 31, no. 22, pp. 1927–1928, Oct. 26, 1995.
- [5] J.-T. Kuo, M. Jiang, and H.-J. Chang, "Design of parallel-coupled microstrip filters with suppression of spurious resonances using substrate suspension," *IEEE Trans. Microw. Theory Tech.*, vol. 52, no. 1, pp. 83–89, Jan. 2004.
- [6] J.-T. Kuo and M. Jiang, "Enhanced microstrip filter design with a uniform dielectric overlay for suppressing the second harmonic response," *IEEE Microw. Wireless Compon. Lett.*, vol. 14, no. 9, pp. 419–421, Sep. 2004.
- [7] T. Lopetegí, M. A. G. Laso, J. Hernández, M. Bacaicoa, D. Benito, M. J. Garde, M. Sorolla, and M. Guglielmi, "New microstrip 'wiggly-line' filters with spurious passband suppression," *IEEE Trans. Microw. Theory Tech.*, vol. 49, no. 9, pp. 1593–1598, Sep. 2001.
- [8] J.-T. Kuo, W.-H. Hsu, and W.-T. Huang, "Parallel coupled microstrip filters with suppression of harmonic response," *IEEE Microw. Wireless Compon. Lett.*, vol. 12, no. 10, pp. 383–385, Oct. 2002.
- [9] S.-F. Chang, Y.-H. Jeng, and J.-L. Chen, "Tapped wiggly-coupled technique applied to microstrip bandpass filters for multioctave spurious suppression," *Electron. Lett.*, vol. 40, no. 1, pp. 46–47, Jan. 8, 2004.
- [10] B. S. Kim, J. W. Lee, and M. S. Song, "Modified microstrip filters improving the suppression performance of harmonic signals," in *IEEE MTT-S Int. Microwave Symp. Dig.*, vol. 1, Jun. 2003, pp. 539–542.
- [11] J. García-García, F. Martín, F. Falcone, J. Bonache, I. Gil, T. Lopetegí, M. A. G. Laso, M. Sorolla, and R. Marqués, "Spurious passband suppression in microstrip coupled line band pass filters by means of split ring resonators," *IEEE Microw. Wireless Compon. Lett.*, vol. 14, no. 9, pp. 416–418, Sep. 2004.
- [12] P. Vincent, J. Culver, and S. Eason, "Meandered line microstrip filter with suppression of harmonic passband response," in *IEEE MTT-S Int. Microwave Symp. Dig.*, vol. 3, Jun. 2003, pp. 1905–1908.
- [13] M. C. Velazquez-Ahumada, J. Martel, and F. Medina, "Parallel coupled microstrip filters with ground-plane aperture for spurious band suppression and enhanced coupling," *IEEE Trans. Microw. Theory Tech.*, vol. 52, no. 3, pp. 1082–1086, Mar. 2004.
- [14] S. Sun and L. Zhu, "Guided-wave characteristics of periodically nonuniform coupled microstrip lines—Even and odd modes," *IEEE Trans. Microwave Theory Tech.*, vol. 53, no. 4, pp. 1221–1227, Apr. 2005.
- [15] L. Zhu, H. Bu, and K. Wu, "Broadband and compact multipole microstrip bandpass filters using ground plane aperture technique," *Proc. Inst. Elect. Eng.*, pt. H, vol. 149, no. 1, pp. 71–77, Feb. 2002.
- [16] G. I. Zysman and A. K. Johnson, "Coupled transmission line networks in an inhomogeneous dielectric medium," *IEEE Trans. Microw. Theory Tech.*, vol. MTT-17, no. 10, pp. 753–759, Oct. 1969.



**Sheng Sun** (S'02) received the B.Eng. degree in information engineering from Xi'an Jiaotong University, Xi'an, China, in 2001, and is currently working toward the Ph.D. degree in microwave engineering at Nanyang Technological University, Singapore.

His research interests include the study of full-wave modeling of planar integrated circuits and antennas, as well as numerical deembedding techniques.

Mr. Sun was the recipient of the Nanyang Technological University Scholarship Award for his Ph.D. research (2002–2005) and the Young Scientist Travel Grant (YSTG) presented at the 2004 International Symposium on Antennas and Propagation (ISAP'04), Sendai, Japan.



**Lei Zhu** (S'91–M'93–SM'00) was born in Wuxi, Jiangsu Province, China, in June 1963. He received the B.Eng. and M.Eng. degrees in radio engineering from the Nanjing Institute of Technology (now Southeast University), Nanjing, China, in 1985 and 1988, respectively, and the Ph.D. Eng. degree in electronic engineering from the University of Electro-Communications, Tokyo, Japan, in 1993.

From 1993 to 1996, he was a Research Engineer with Matsushita-Kotobuki Electronics Industries Ltd., Tokyo, Japan. From 1996 to 2000, he was a

Research Fellow with the École Polytechnique de Montréal, University of Montréal, Montréal, QC, Canada. Since July 2000, he has been an Associate Professor with the School of Electrical and Electronic Engineering, Nanyang Technological University, Singapore. His current research interests include the study of planar integrated dual-mode filters, ultra-broad bandpass filters, broad-band interconnects, planar periodic structures, planar antenna elements/arrays, uniplanar coplanar waveguide (CPW)/coplanar stripline (CPS) circuits, as well as full-wave method of moments (MoM) modeling of planar integrated circuits and antennas, numerical deembedding or parameter-extraction techniques, field-theory computer-aided design (CAD) synthesis, and optimization design procedures. He is currently an Associate Editor for the *IEICE Transactions on Electronics*.

Dr. Zhu is currently an Editorial Board member for the IEEE TRANSACTIONS ON MICROWAVE THEORY AND TECHNIQUES. He was the recipient of the Japanese Government (Monbusho) Graduate Fellowship (1989–1993), the First-Order Achievement Award in Science and Technology from the National Education Committee in China (1993), the Silver Award of Excellent Invention from the Matsushita-Kotobuki Electronics Industries Ltd., Japan (1996), and the Asia-Pacific Microwave Prize Award presented at the 1997 Asia-Pacific Microwave Conference, Hong Kong.